



# Ceria promoted Pd/C catalysts for glucose electrooxidation in alkaline media



Shuqin Song<sup>a</sup>, Kun Wang<sup>a</sup>, Longlong Yan<sup>a</sup>, Angeliki Brouzgou<sup>c,d</sup>, Yueli Zhang<sup>a,\*,\*\*</sup>,  
Yi Wang<sup>b,\*,\*\*</sup>, Panagiotis Tsiakaras<sup>c,d,\*</sup>

<sup>a</sup> State Key Laboratory of Optoelectronic Materials and Technologies/The Key Lab of Low-carbon Chemistry and Energy Conservation of Guangdong Province, School of Physics and Engineering, Sun Yat-sen University, Guangzhou 510275, China

<sup>b</sup> The Key Lab of Low-Carbon Chemistry & Energy Conservation of Guangdong Province, School of Chemistry and Chemical Engineering, Sun Yat-sen University, Guangzhou 510275, China

<sup>c</sup> Laboratory of Electrochemical Devices Based on Solid Oxide Proton Electrolytes, Institute of High Temperature Electrochemistry, Russian Academy of Sciences, 620990 Yekaterinburg, Russia

<sup>d</sup> Laboratory of Alternative Energy Conversion Systems, Department of Mechanical Engineering, School of Engineering, University of Thessaly, Pedion Areos 38834, Greece

## ARTICLE INFO

### Article history:

Received 22 January 2015

Received in revised form 25 March 2015

Accepted 31 March 2015

Available online 1 April 2015

### Keywords:

Glucose electrooxidation

Pd/CeO<sub>2</sub>-C catalyst

Microwave assisted polyol method

Alkaline media

## ABSTRACT

Carbon support materials are modified by CeO<sub>2</sub> through a microwave decomposition method, and then CeO<sub>2</sub>-C supported Pd catalysts are synthesized by a pulse microwave assisted polyol method. The content of CeO<sub>2</sub> is appropriately adjusted and Pd/CeO<sub>2</sub>-C catalysts with different Pd:CeO<sub>2</sub> molar ratios are obtained and investigated for the reaction of glucose electrooxidation in alkaline media.

It is found that the introduction of CeO<sub>2</sub> onto the surface of the carbon support can significantly decrease the particle size of Pd with respect to the Pd/C case, generating sufficient OH<sub>ads</sub> at lower potentials. Accordingly, the catalytic activity of Pd for glucose electrooxidation can be improved as a result of its high dispersion and the synergistic effect. It is also found that, among the Pd/CeO<sub>2</sub>-C catalysts, the one with Pd:CeO<sub>2</sub> molar ratio of 3:1 exhibits the best performance for glucose electrooxidation, ~30% higher than that of Pd/C. Moreover, the optimized catalyst presents the advantages of rapid response, high sensitivity and good tolerance to the interfering agents co-existing in the human blood with glucose.

© 2015 Elsevier B.V. All rights reserved.

## 1. Introduction

Ceria (CeO<sub>2</sub>), possessing unique properties of oxygen storage property, surface basicity, electrochemical redox reaction between Ce<sup>4+</sup> and Ce<sup>3+</sup> in cerium oxide lattice, and the ability as an oxygen buffer [1,2], has been adopted as the promoter for Pt or Pd toward alcohol electrooxidation [3–7]. The enhanced electrode performance (reaction activity and poison resistance) for alcohols electrooxidation was attributed to the synergistic effect of CeO<sub>2</sub> by supplying sufficient OH<sub>ads</sub> at lower potentials, which is necessary to eliminate the poisoning species adsorbed on Pt or Pd active sites [4,5]. Moreover, the promoting effect of CeO<sub>2</sub> can also be due to its oxygen storage capacity at low temperature, higher reducibility

in the presence of Pt, high dispersion of Pt on CeO<sub>2</sub> and prevention of agglomeration of Pt metal particles [8]. Moreover, CeO<sub>2</sub> can increase the dispersion of the active metal on the support surface [9], and in this way increase the metal utilization coefficient and its specific activity.

Glucose electrooxidation reaction (GOR) has recently received a great attention mainly due to its potential applications in both control and treatment of diabetes through an electrochemical glucose sensor, and the implantable direct glucose fuel cells for artificial hearts and heart pacer [10–13]. Among the different tentative candidates as the electrocatalysts for glucose electrooxidation, Pd based catalysts exhibited high activity, desirable stability, and high selectivity [14–19]. On the other hand, the poison problem still exists with Pd alone as the catalyst. Furthermore, the supported Pd catalysts, not like Pt, have a poor dispersion, with much bigger particle size than that of Pt with the similar catalyst preparation process [19,20]. Ammonia adjustment for Pd preparation through glycol reduction method can decrease the Pd particle size a little [17,21], but its dispersion needs further improvement for exploring

\* Corresponding author. Tel.: +30 24210 74065; fax: +30 24210 74050.

\*\* Corresponding author. Tel.: +86 20 841 10930; fax: +86 20 841 13253.

\*\*\*Corresponding author. Tel.: +86 20 841 13398; fax: +86 20 841 13397.

E-mail addresses: [stszy@mail.sysu.edu.cn](mailto:stszy@mail.sysu.edu.cn)

(Y. Zhang), [wangyi76@mail.sysu.edu.cn](mailto:wangyi76@mail.sysu.edu.cn) (Y. Wang), [tsiak@uth.gr](mailto:tsiak@uth.gr) (P. Tsiakaras).

its capability for glucose electrooxidation. In order to take advantage of both the electrocatalytic property of Pd toward glucose electrooxidation and the synergistic function of CeO<sub>2</sub> and its possible role in catalyst preparation for decreasing metal particle size, before Pd deposition, CeO<sub>2</sub> is designed to be firstly decorate the carbon supporting materials.

In the present investigation, the promoting effect of CeO<sub>2</sub> on Pd catalyst toward glucose electrooxidation in alkaline media and the optimization of CeO<sub>2</sub> content in the catalyst were investigated. The composite catalysts were prepared by firstly depositing CeO<sub>2</sub> onto Vulcan XC-72R carbon black by a microwave deposition process and then depositing Pd through a pulse microwave assisted polyol method. Glucose electrooxidation on the as-prepared Pd/CeO<sub>2</sub>-C series catalyst was evaluated by cyclic voltammetry and chronoamperometry in alkaline media.

## 2. Experimental

### 2.1. Materials

Glucose (Guangzhou Chemical Reagent Corp., AR), NH<sub>3</sub>·H<sub>2</sub>O (Guangzhou Chemical Reagent Corp., 25 wt%), Ce(NO<sub>3</sub>)<sub>3</sub>·6H<sub>2</sub>O, carbon black (Vulcan XC-72R, Cabot Corp.), PdCl<sub>2</sub> (Guiyanboye Corp., AR), ethylene glycol (Shanghai Lingfeng Corp., AR), Nafion solution (DuPont Company, 5 wt%) were used without further purification. All the other used chemicals were of analytical reagent grade. Deionized water with specific resistance more than 18.0 MΩ cm<sup>-1</sup> was obtained by a water purification system.

### 2.2. Preparation of Pd/CeO<sub>2</sub>-C catalysts

Vulcan XC-72 R carbon black was modified by CeO<sub>2</sub> via the precipitation method. For a typical preparation process, according to the pre-calculated feeding weight ratio, Ce(NO<sub>3</sub>)<sub>3</sub>·6H<sub>2</sub>O was dissolved in the mixed solution containing 15.0 mL distilled water and 15.0 mL isopropanol. After carbon black was well dispersed into the above solution, NH<sub>3</sub>·H<sub>2</sub>O was added drop by drop until the pH value was more than 9.0. The precipitation was aged in the mother solution for 3 h, followed by filtering, washing, and then drying at 80 °C in a vacuum oven for 12 h. The obtained powder was microwave-heated (Nanjinghuiyan Corp., MZG800S) for 3 min continuously to obtain CeO<sub>2</sub>-C with different CeO<sub>2</sub> content.

The Pd/CeO<sub>2</sub>-C catalysts with different Pd/CeO<sub>2</sub> molar ratios were prepared by a pulse microwave assisted polyol method [19]. The as-prepared CeO<sub>2</sub>-C as the supporting materials (120.0 mg) was well mixed with ethylene glycol (EG) in an ultrasonic bath and then 2.50 mL of 12.0 mg mL<sup>-1</sup> Pd<sup>2+</sup>/EG solution was added into the mixture. After the pH value of the above mixture was adjusted to more than 10 by introducing 1.0 mol L<sup>-1</sup> NaOH/EG solution drop by drop, a well-dispersed slurry was obtained with magnetic stirring for another 1 h. Then, the slurry was heated in a microwave oven (Nanjinghuiyan Corp., MZG800S) in the pulse form of 10 s-ON/10 s-OFF for several times. After reaction, 1.0 mol L<sup>-1</sup> HCl solution was added to accelerate the deposition process. Finally, the resulting sample was filtered, washed with copious hot water (≥80 °C) until no chloride anion was detected in the filtrate by 1.0 mol L<sup>-1</sup> AgNO<sub>3</sub> solution and then dried at 90 °C overnight in a vacuum oven. In all the catalysts, the theoretical Pd loading was 20 wt%. The molar ratios of Pd to CeO<sub>2</sub> in the Pd/CeO<sub>2</sub>-C-x samples were controlled to be 1–5, and the corresponding samples were denoted as Pd/CeO<sub>2</sub>-C-1, Pd/CeO<sub>2</sub>-C-2, Pd/CeO<sub>2</sub>-C-3, Pd/CeO<sub>2</sub>-C-4, and Pd/CeO<sub>2</sub>-C-5, respectively. For the sake of one-to-one correspondence to the support materials, the corresponding used CeO<sub>2</sub>-C samples were denoted as CeO<sub>2</sub>-C-1, CeO<sub>2</sub>-C-2, CeO<sub>2</sub>-C-3, CeO<sub>2</sub>-C-4 and CeO<sub>2</sub>-C-5, respectively. In CeO<sub>2</sub>-C-x samples, their

respective CeO<sub>2</sub> weight percentage were 35.86 wt% for CeO<sub>2</sub>-C-1, 17.93 wt% for CeO<sub>2</sub>-C-2, 11.95 wt% for CeO<sub>2</sub>-C-3, 8.96 wt% for CeO<sub>2</sub>-C-4 and 7.17 wt% for CeO<sub>2</sub>-C-5.

### 2.3. Physico-chemical and electrochemical characterization

The samples were characterized by X-ray powder diffraction (XRD) (Rigaku Co., Japan) with Cu Kα radiation (40 kV, 40 mA). The chemical composition of the obtained products was determined by scanning electron microscopy with energy dispersive X-ray spectroscopy (SEM-EDX) (JEOL JSM-6330F). For the determination of metal content in the catalysts, thermogravimetric (TG) experiments were carried out by the aid of a Netzsch TG-209 analyzer in air with a flow rate of 50 mL min<sup>-1</sup> and a temperature ramp of 10 °C min<sup>-1</sup>.

Electrochemical measurements were carried out using an AUT84480 instrument in a three-electrode electrochemical cell at 36.5 °C. Hg/HgO electrode (0.1 mol L<sup>-1</sup> KOH) and platinum foil (1.0 cm × 1.0 cm) were adopted as the reference and the counter electrodes, respectively. The working electrode was prepared by dispersing 5.0 mg of the as-prepared catalyst powder in 1.80 mL ethanol and 0.20 mL Nafion solution. The suspension was sonicated and stirred for ca. 30 min. Then, 10 μL of this ink was transferred onto the surface of the glassy carbon electrode with a diameter of 0.5 cm, and then the electrode was dried by an infrared lamp. The electrochemical tests of cyclic voltammetry (CV) and chronoamperometry (CA) were performed in an aqueous solution containing 0.1 mol L<sup>-1</sup> NaOH and 20.0 mmol L<sup>-1</sup> glucose. Before measurements, the electrolyte solution was saturated with high-purity N<sub>2</sub> gas to remove the dissolved oxygen and provide an inert atmosphere. It should be noted that without specification, all the potentials are referred to Hg/HgO (0.1 mol L<sup>-1</sup> KOH) reference electrode.

## 3. Results and discussion

The XRD patterns of CeO<sub>2</sub>-C samples with different CeO<sub>2</sub> content are schematically shown in Fig. 1. Five diffraction peaks (1 1 1), (2 0 0), (2 2 0), (3 1 1), and (3 3 1) are observed, corresponding to about 28°, 33°, 47°, 56° and 79°, respectively. This result indicates that CeO<sub>2</sub> exists in the form of cubic fluorite structure, which is in good agreement with the reported values [22,23]. Moreover, with the content of CeO<sub>2</sub> increasing in the composite samples, the inten-

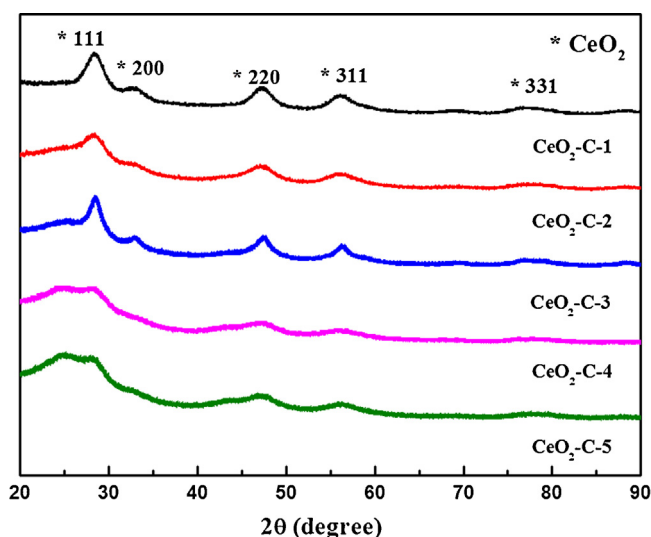


Fig. 1. XRD patterns for CeO<sub>2</sub>-C samples. 2θ scanning range: 20–90° at a scan rate of 10° min<sup>-1</sup>.

sity of diffraction patterns of  $\text{CeO}_2$  becomes stronger. In the lowest content of  $\text{CeO}_2$  ( $\text{CeO}_2$ -C-5), the diffraction peaks at high  $2\theta$  values are not obvious.

After depositing Pd onto  $\text{CeO}_2$ -C, three characteristic diffraction peaks at  $2\theta = 40^\circ$ ,  $68^\circ$ , and  $82^\circ$  are also observed, corresponding to the (1 1 1), (2 2 0) and (3 1 1) crystalline planes of the face-centered cubic (fcc) structure of Pd, respectively (Fig. 2A). The diffraction peaks of Pd in Pd/ $\text{CeO}_2$ -C catalysts are shifted to the higher  $2\theta$  angle with respect to those in Pd/C, which could result from the interaction between Pd and  $\text{CeO}_2$ . The Pd particle size can be calculated from the Pd (2 2 0) fine diffraction peaks, shown in Fig. 2B, by using the Scherrer formula [24]. The crystallite sizes are 3.1, 3.4, 3.7, 3.9 and 4.4 nm for Pd/ $\text{CeO}_2$ -C-1, Pd/ $\text{CeO}_2$ -C-2, Pd/ $\text{CeO}_2$ -C-3, Pd/ $\text{CeO}_2$ -C-4, and Pd/ $\text{CeO}_2$ -C-5, respectively, which are much lower than that of Pd/C (12.6 nm) [19]. In other words, the introduction of  $\text{CeO}_2$  can decrease the Pd particle size and improve the dispersion compared with Pd/C counterpart. This behavior could be attributed to the negative charges of  $\text{CeO}_2$  particles in the case of  $\text{pH} > 7.8$  (in the present investigation for catalyst preparation process, pH value is larger than 10) [25,26]. Accordingly, through electrostatic attraction,  $\text{CeO}_2$  with negative charges are easily to be

**Table 1**Physico-chemical properties of the as-prepared Pd/ $\text{CeO}_2$ -C catalysts.

Samples	Mean particle size/nm	Pd/Ce atomic ratio		Pd content (wt%) (TG)
		EDS	Feeding ratio <sup>a</sup>	
Pd/ $\text{CeO}_2$ -C-1	3.1	51/49	1/1	20.0
Pd/ $\text{CeO}_2$ -C-2	3.4	68/32	2/1	20.7
Pd/ $\text{CeO}_2$ -C-3	3.7	74/26	3/1	19.4
Pd/ $\text{CeO}_2$ -C-4	3.9	78/22	4/1	19.7
Pd/ $\text{CeO}_2$ -C-5	4.4	83/17	5/1	18.6

<sup>a</sup> Here, in Pd/ $\text{CeO}_2$ -C catalysts, the Pd weight percentage is 20 wt% for all the samples while the feeding ratio between Pd/Ce is different.

deposited onto carbon black support with positive charges. Due to the oxygen species provided by  $\text{CeO}_2$ , the surface of carbon black could be functionalized with hydroxyl and carbonyl groups, which can act as the anchoring sites for metal particles [27].

The composite and the Pd loading of the as-prepared Pd/ $\text{CeO}_2$ -C series catalysts were characterized by SEM-EDS and TG. The EDS results (Fig. 3A–E and A'–E') (as summarized in Table 1) show that the respective Pd/ $\text{CeO}_2$  atomic ratio are 51/49, 68/32, 74/26, 78/22, 83/17 for Pd/ $\text{CeO}_2$ -C-1, Pd/ $\text{CeO}_2$ -C-2, Pd/ $\text{CeO}_2$ -C-3, Pd/ $\text{CeO}_2$ -C-4, and Pd/ $\text{CeO}_2$ -C-5. These values were very close to the corresponding feeding weight ratio. Based on the above EDS results, the Pd content in the catalysts was determined by TG [19]. As shown in Fig. 4, below 200 °C, the weight loss for catalysts could be attributed to the desorption of water vapor and the residual EG. Therefore, the metal loading in the catalysts can be calculated from their TG curves after subtracting the weight of adsorbed water and residual EG. The results are 20.0, 20.7, 19.4, 19.7 and 18.6 wt% for Pd/ $\text{CeO}_2$ -C-1, Pd/ $\text{CeO}_2$ -C-2, Pd/ $\text{CeO}_2$ -C-3, Pd/ $\text{CeO}_2$ -C-4, and Pd/ $\text{CeO}_2$ -C-5, respectively, which are basically in accordance with their feeding weight ratios (20.0 wt%).

To further understand the effect of  $\text{CeO}_2$  and Pd interaction in the as-prepared samples, XPS spectra were collected for Pd/C and Pd/ $\text{CeO}_2$ -C-3 catalysts. Their corresponding XPS spectra for Pd 3d and Ce 3d are shown in Fig. 5. For both samples, the Pd 3d peak can be deconvoluted into some pairs of doublets, as shown in Fig 5A and B. From the relative areas of the integrated intensity of the Pd and PdO peaks in Pd/C and Pd/ $\text{CeO}_2$ -C-3, it is found that the percentage composition of  $\text{Pd}^0$  (Table 2) decreases from 71.44% in Pd/C to 46.52% in Pd/ $\text{CeO}_2$ -C-3, while the corresponding value of  $\text{Pd}^{2+}$  in the form of PdO increases from 28.57 to 41.90% after  $\text{CeO}_2$

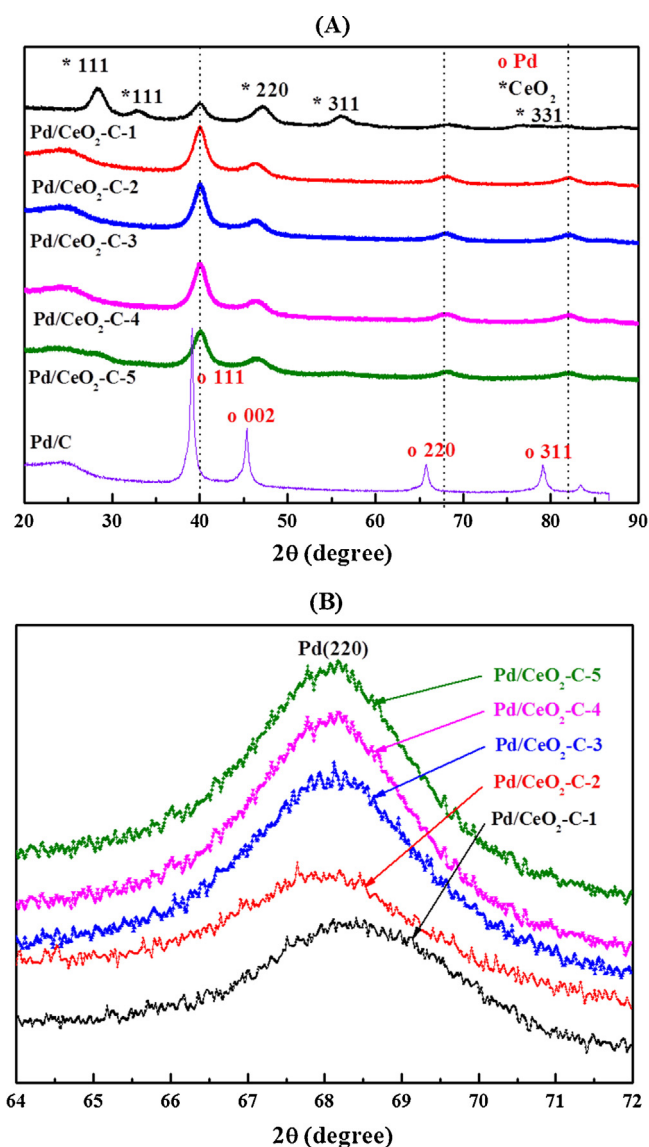


**Fig. 2.** XRD patterns for Pd/ $\text{CeO}_2$ -C catalysts.  $2\theta$  scanning range:  $20\text{--}90^\circ$  at a scan rate of  $10^\circ \text{ min}^{-1}$  (A), and  $2\theta$  scanning range:  $64\text{--}72^\circ$  at a scan rate of  $1^\circ \text{ min}^{-1}$  (B).

**Table 2**Binding energies and surface compositions from deconvolution of XPS spectra for Pd/C and Pd/ $\text{CeO}_2$ -C-3 catalysts.

Catalyst	Peak	Binding Energy (eV)	Species	Relative ratio (%)
Pd/C	Pd 3d	335.62	Pd metal	39.21
		341	Pd metal	32.23
		336.62	PdO	16.96
		342.52	PdO	11.61
Pd/ $\text{CeO}_2$ -C-3	Pd 3d	335.68	Pd metal	28.63
		340.9	Pd metal	17.62
		336.59	PdO	23.56
		341.8	PdO	17.34
		337.74	$\text{Pd}_x\text{Ce}_y\text{O}_z$	7.47
	Ce 3d	343.01	$\text{Pd}_x\text{Ce}_y\text{O}_z$	5.38
		883.41	$\text{CeO}_2$	25.98
		886.69	$\text{Ce}_2\text{O}_3$	13.74
		889.7	$\text{CeO}_2$	2.5
		890.2	$\text{CeO}_2$	2.38
		898.86	$\text{Pd}_x\text{Ce}_y\text{O}_z$	15.79
		901.64	$\text{CeO}_2$	9.95
		904.43	$\text{Ce}_2\text{O}_3$	17.85
		917.35	$\text{CeO}_2$	11.82

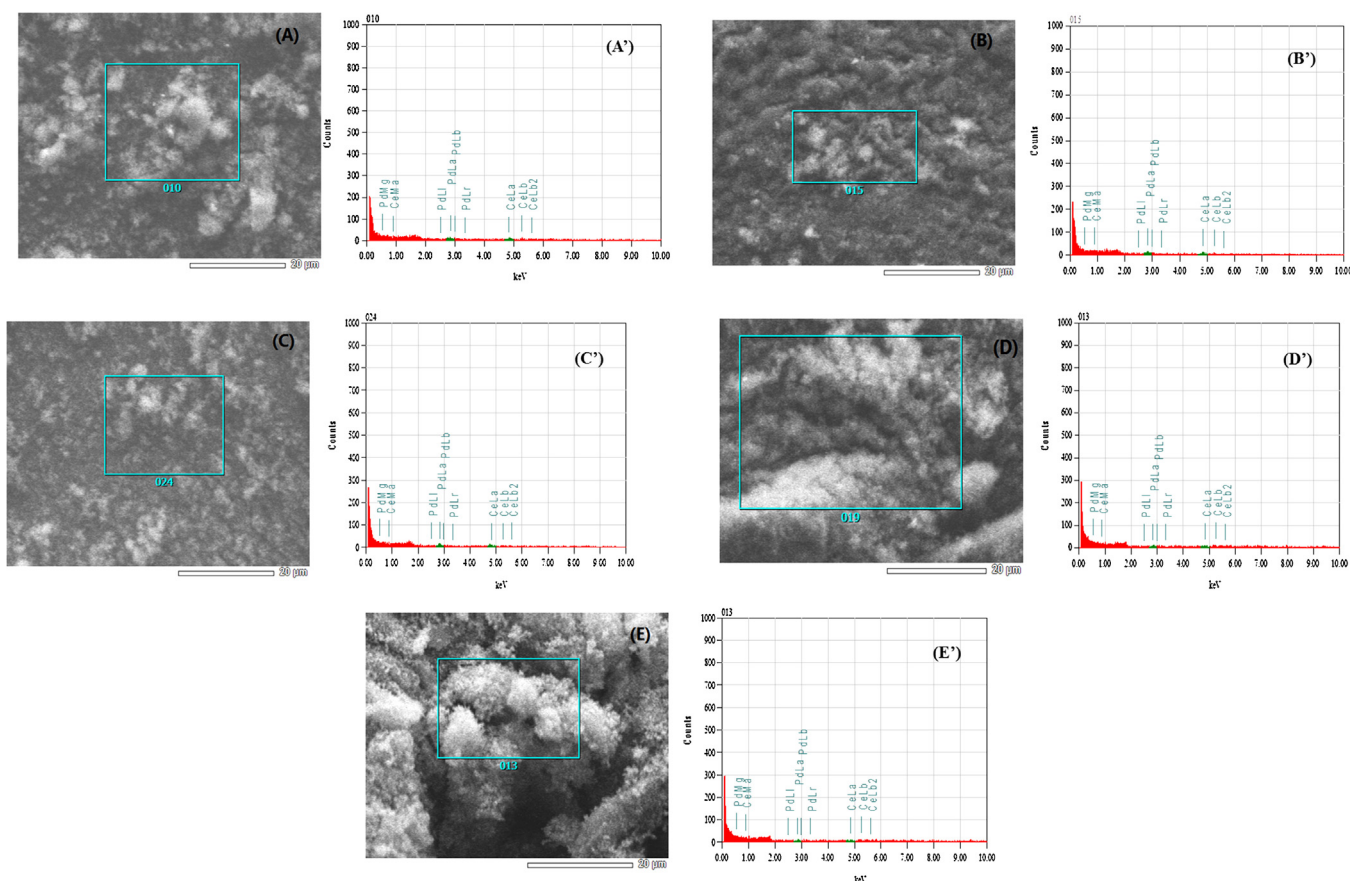


Fig. 3. SEM images of Pd/CeO<sub>2</sub>-C-1 (A), Pd/CeO<sub>2</sub>-C-2 (B), Pd/CeO<sub>2</sub>-C-3 (C), Pd/CeO<sub>2</sub>-C-4 (D), Pd/CeO<sub>2</sub>-C-5 catalysts (E) and their corresponding EDS results (A'–E').

is introduced into Pd/C. Obviously, CeO<sub>2</sub> can significantly increase the relative percentage composition of PdO in Pd/CeO<sub>2</sub>-C-3 catalyst due to oxygen species provided by CeO<sub>2</sub>. The existence of Pd<sub>x</sub>Ce<sub>y</sub>O<sub>z</sub> peaks in Fig. 5B and C indicates that Pd and CeO<sub>2</sub> form the compound in the preparation process of Pd/CeO<sub>2</sub>-C-3 catalyst. For Ce 3d peaks shown in Fig. 5C, there are some feature peaks to depict the chemical state of Ce element, and the main peaks located at 883.41, 889.70, 890.20, 901.64 and 917.35 eV are typical of Ce<sup>4+</sup> [28]. Concerning Ce<sup>3+</sup>, the peaks located at 886.69 and 904.43 eV are its typical peaks. The percentage composition of Ce<sup>4+</sup> is 42.68%, showing the main composition, while that of Ce<sup>3+</sup> is 31.59%. The Pd 3d peaks of Pd/CeO<sub>2</sub>-C-3 (Fig. 5B) are shifted to higher binding energies (335.68 and 340.90 eV) relative to those of Pd/C (335.62 and 341.00 eV), indicating a strong interaction between CeO<sub>2</sub> and Pd due to the change of the electronic states of the Pd atoms, similar to the case of Pt [4,29].

In Fig. 6 the CV curves of glucose electrooxidation on Pd/CeO<sub>2</sub>-C catalysts with different CeO<sub>2</sub> contents in an aqueous solution containing 1.0 mol L<sup>-1</sup> KOH and 20.0 mmol L<sup>-1</sup> glucose with a potential scanning rate of 50 mV s<sup>-1</sup> at 36.5 °C, are depicted. In the forward potential scanning, the oxidation peak at about 0.02 V for all the catalysts can be attributed to either the oxidation of glucose on the surface of the catalyst or the further oxidation of adsorbed species at more positive potential, which is an indicator of the activity of the catalysts. The higher current density is, the better catalysts are. Obviously, the CeO<sub>2</sub> content in the Pd/CeO<sub>2</sub>-C catalysts has a considerable effect on the electrocatalytic activity for glucose oxidation. Its corresponding effect can be distinctly observed in Fig. 6B. With the increase of CeO<sub>2</sub> content until the Pd:CeO<sub>2</sub> molar ratio is 3, the current density increases from 4.4 mA cm<sup>-2</sup> on Pd/C to 5.7 mA cm<sup>-2</sup> on Pd/CeO<sub>2</sub>-C-3, which is even higher

than that on Pd-based binary catalysts [17–19,30]. While a further increase of the CeO<sub>2</sub> content in the Pd/CeO<sub>2</sub>-C catalysts leads to the decrease of the current density, and even worse than that on Pd/C. The above volcano behavior with Pd/CeO<sub>2</sub>-C-3 at the summit could be understood as follows. The performance enhancement is attributed to the decreased Pd particles size as CeO<sub>2</sub> is introduced as proved by XRD results and the synergistic of CeO<sub>2</sub> to remove the adsorbed intermediate products as oxygen storage materials [31,32]. While, the excessive amount of CeO<sub>2</sub> results

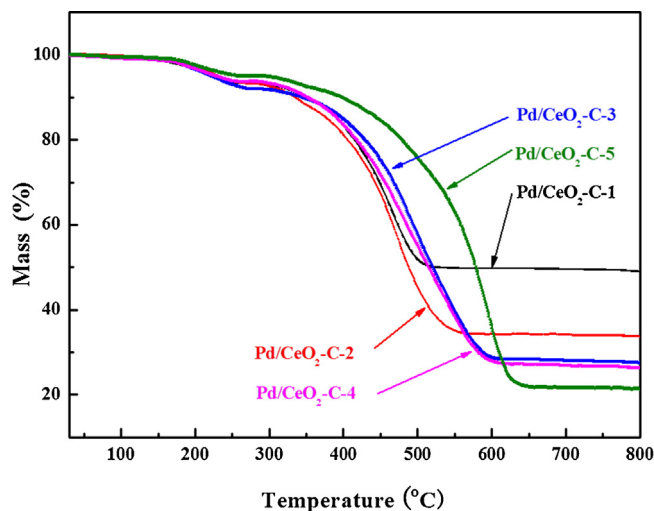


Fig. 4. Thermogravimetric curves of Pd/CeO<sub>2</sub>-C catalysts.

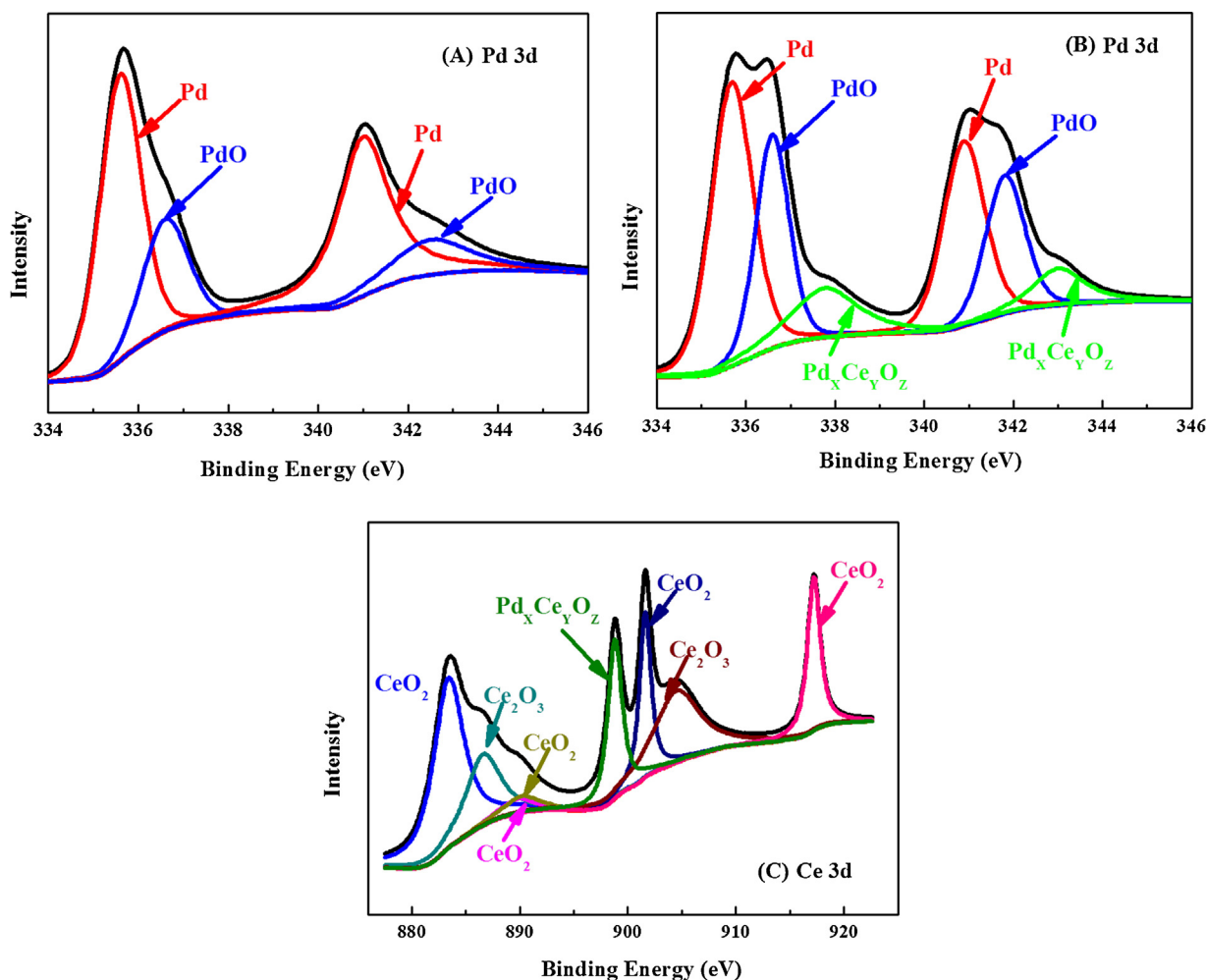


Fig. 5. XPS spectra for Pd 3d of the Pd/C catalyst (A), and Pd 3d (B) and Ce 3d (C) of the Pd/CeO<sub>2</sub>-C-3 catalyst.

in the decayed current density because of both the decrease of the electrical conductivity and partial blockage of the Pd active sites.

For the potential application in the electrochemical sensors, electrocatalysts are generally evaluated by monitoring the current response vs. time at a fixed applied potential after the addition of the analyte and possible interfering agents [33,34]. To assess the electrochemical response of Pd/CeO<sub>2</sub>-C-3 for glucose electrooxidation, a chronoamperometric test was carried out on a rotating disk electrode (1600 rpm) at 0.02 V by a successive addition of the analyte (1.0 mmol L<sup>-1</sup> glucose each time) into 0.1 mol L<sup>-1</sup> NaOH solution at a regular interval time of 60 s. As shown in Fig. 7, once 1.0 mmol L<sup>-1</sup> glucose is injected into 0.1 mol L<sup>-1</sup> NaOH solution, the current sharply increases and then levels off to a relatively constant value. The corresponding calibration plot for current vs. glucose concentration is linear in the investigated glucose concentration range from 1.0 to 10.0 mmol L<sup>-1</sup> with a slope of 3.454  $\mu$ A mM<sup>-1</sup>. The measure of goodness-of-fit of linear regression ( $R^2$ ) is found to be 0.99975, indicating a very good linear relationship between the response current and glucose concentration in the investigated range. Anti-interference ability should be considered for the electrochemical sensor in detecting diabetes. The electrochemical response of the interfering species was investigated on Pd/CeO<sub>2</sub>-C-3 with the successive injection of analyte (1.0 mmol L<sup>-1</sup> glucose) and interfering agents including 0.1 mM dopamine (DA), 0.1 mmol L<sup>-1</sup> uric acid (UA), 0.1 mmol L<sup>-1</sup>

ascorbic acid (AA), 0.1 mmol L<sup>-1</sup> fructose, 0.1 mmol L<sup>-1</sup> sucrose, 0.1 mmol L<sup>-1</sup> sodium gluconate, 0.1 mmol L<sup>-1</sup> glucolactone, and 0.15 mol L<sup>-1</sup> NaCl. The above species and concentrations are chosen based on the consideration that they are co-existing species with glucose in human blood and their corresponding concentrations except that NaCl is about one thirtieth of glucose concentration. As shown in Fig. 8, once the glucose is injected, a quick increase in current is observed, which is consistent with the results depicted in Fig. 7. While with the further successive injection of the interfering agents including DA, AA and UA, fructose, sucrose, sodium gluconate, glucolactone, and NaCl at a regular interval time of 60 s, the current response is insignificant. After this series of injection, with another injection of 1.0 mmol L<sup>-1</sup> glucose, the corresponding current increases sharply again. It can be inferred that the small quality of DA, AA and UA, fructose, sucrose, sodium gluconate, glucolactone, and 0.15 mol L<sup>-1</sup> NaCl does not interfere the detection of glucose through electrochemical process. In other words, Pd/CeO<sub>2</sub>-C-3 exhibits high selectivity to glucose detection and good poison tolerance to Cl<sup>-</sup>.

The long-term performance of the electrocatalyst was studied by chronoamperometric measurement. The chronoamperometric profiles of glucose oxidation on Pd/CeO<sub>2</sub>-C-3 and Pd/C electrocatalysts at 0.2 V are shown in Fig. 9. The initial current of Pd/CeO<sub>2</sub>-C-3 is twice larger than that on Pd/C, indicating a higher catalytic activity. The current on Pd/CeO<sub>2</sub>-C-3 decreases more slowly than on Pd/C, implying Pd/CeO<sub>2</sub>-C-3 presents a higher stability. This

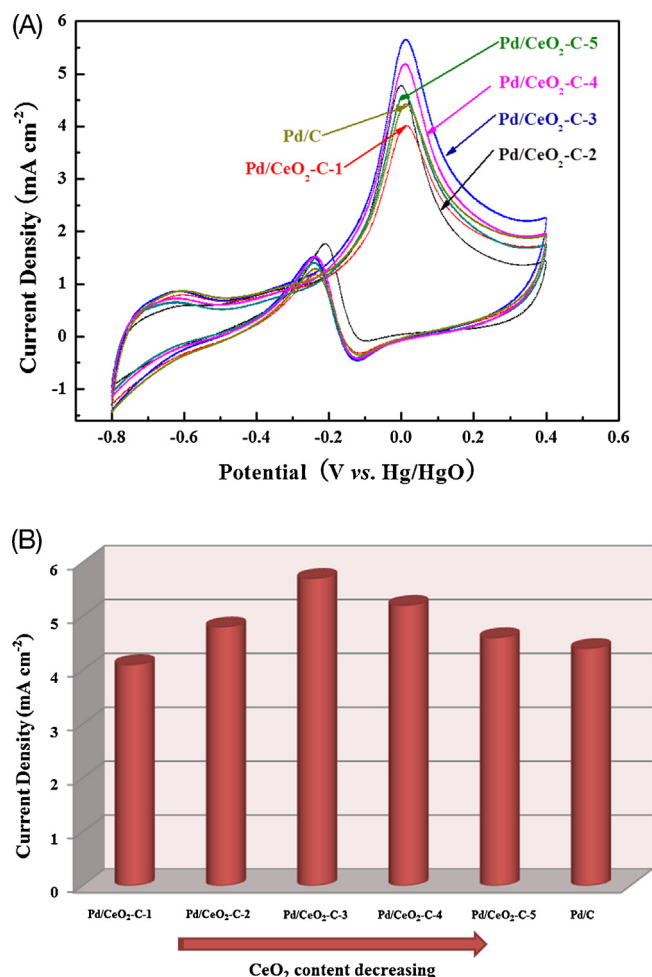


**Fig. 6.** Cyclic voltammograms of Pd/CeO<sub>2</sub>-C in 0.1 mol L<sup>-1</sup> NaOH aqueous solution in the presence of 20.0 mmol L<sup>-1</sup> glucose at 50 mV s<sup>-1</sup> and at 36.5 °C (A) and their corresponding peak current densities on different catalysts (B).

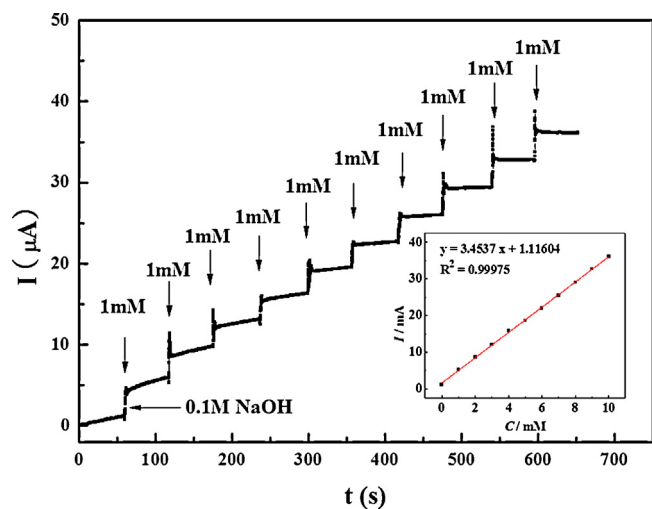


**Fig. 7.** Current-time record of glucose electrooxidation on Pd/CeO<sub>2</sub>-C-3 catalyst fixed onto RDE (1600 rpm) by successively injecting 1.0 mmol L<sup>-1</sup> glucose into 0.1 mol L<sup>-1</sup> NaOH solution at a regular interval time of 60 s. Applied potential: 0.02 V (vs. Hg/HgO electrode). Inset is the relationship between the current and the added glucose solution.

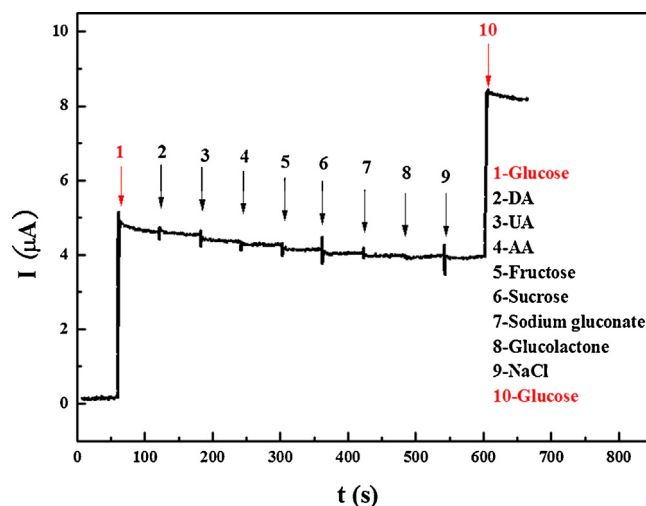


**Fig. 8.** Current-time record of Pd/CeO<sub>2</sub>-C-3 catalyst fixed onto rotating disk electrode (1600 rpm) by successively injecting 1.0 mmol L<sup>-1</sup> glucose, 0.1 mmol L<sup>-1</sup> sodium gluconate, 0.1 mmol L<sup>-1</sup> glucolactone, 0.1 mmol L<sup>-1</sup> fructose, 0.1 mmol L<sup>-1</sup> sucrose, 0.15 mmol L<sup>-1</sup> NaCl and 1.0 mmol L<sup>-1</sup> glucose into 0.1 mol L<sup>-1</sup> NaOH solution at a regular interval time of 60 s. Applied potential: 0.02 V (vs. Hg/HgO electrode).

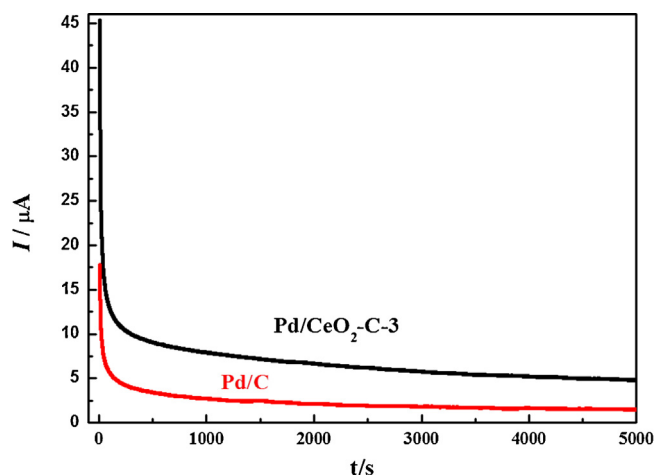


**Fig. 9.** Chronoamperometric curves for glucose electrooxidation in a N<sub>2</sub>-saturated aqueous solution of 0.1 mol L<sup>-1</sup> NaOH and 20.0 mmol L<sup>-1</sup> glucose at 36.5 °C on Pd/C and Pd/CeO<sub>2</sub>-C-3. Applied potential: 0.2 V (vs. Hg/HgO electrode).

result demonstrates that the introduction of CeO<sub>2</sub> improves the electrocatalytic activity and stability of Pd/CeO<sub>2</sub>-C-3 catalyst in comparison with that of Pd/C catalyst.

#### 4. Conclusions

Carbon black was successfully decorated with CeO<sub>2</sub> through the precipitation method followed by microwave heating process. With the composite CeO<sub>2</sub>-C as the support materials, Pd/CeO<sub>2</sub>-C series catalysts were synthesized by a modified pulse microwave assisted polyol method and investigated for glucose electrooxidation and detection. The Pd/CeO<sub>2</sub> molar ratio in Pd/CeO<sub>2</sub>-C catalysts could be controlled and adjusted by changing the corresponding CeO<sub>2</sub> content in CeO<sub>2</sub>-C samples while keeping the same Pd content in Pd/CeO<sub>2</sub>-C.

The introduction of CeO<sub>2</sub> can greatly decrease the Pd particle size and thus increase its dispersion, which is helpful to improve Pd's activity toward glucose electrooxidation.

Together with the synergistic effect of  $\text{CeO}_2$ , the existence of  $\text{CeO}_2$  in the support materials can obviously affect the catalytic activity, with  $\text{Pd/CeO}_2\text{-C-3}$  (the  $\text{Pd/CeO}_2$  molar ratio is 3) exhibiting the best performance for glucose electrooxidation as the comprehensive results of the above contributing effects and decreased conductivity due to  $\text{CeO}_2$ .

$\text{Pd/CeO}_2\text{-C-3}$  also possesses a very sensitive and linear amperometric response for glucose molecules and good tolerance to the interfering agents co-existing in the human blood with glucose.

The fact that the introduction of  $\text{CeO}_2$  can significantly decrease the Pd particles size resulting in the preparation of well dispersed supported Pd materials makes them good candidates in other research areas.

## Acknowledgements

The authors would like to thank the financial support of the National Natural Science Foundation of China (Grant No. 21276290) and the Sino-Greek Science and Technology Cooperation Project (2013DFG62590). We also thank the project of Guangdong Province Nature Science Foundation (2014A030313150). Prof. P. Tsiakaras and Dr Brouzgou are grateful to the Ministry of Education and Science of the Russian Federation (contract No. 14.Z50.31.0001) and to “Bilateral R&D Co-operation between Greece–China 2012–2014”, co-financed by the European Union and the Greek Ministry of Education-GSRT, for financial support.

## References

- [1] T. Mori, D.R. Ou, J. Zou, J. Drennan, *Prog. Nat. Sci. Mater.* 22 (2012) 561–571.
- [2] C. Perkins, M. Henderson, C. Peden, G. Herman, *J. Vac. Sci. Technol. A* 19 (2001) 1942–1946.
- [3] M.A. Scibioh, S.K. Kim, E.A. Cho, T.H. Lim, S.A. Hong, H.Y. Ha, *Appl. Catal. B: Environ.* 84 (2008) 773–782.
- [4] D.M. Gu, Y.Y. Chu, Z.B. Wang, Z.Z. Jiang, G.P. Yin, Y. Liu, *Appl. Catal. B: Environ.* 102 (2011) 9–18.
- [5] C.W. Xu, R. Zeng, P.K. Shen, Z.D. Wei, *Electrochim. Acta* 51 (2005) 1031–1035.
- [6] H. Chen, J. Duan, X. Zhang, Y. Zhang, C. Guo, L. Nie, X. Liu, *Mater. Lett.* 126 (2014) 9–12.
- [7] K.H. Ye, S.A. Zhou, X.C. Zhu, C.W. Xu, P.K. Shen, *Electrochim. Acta* 90 (2013) 108–111.
- [8] P. Bera, A. Gayen, M.S. Hegde, N.P. Lalla, L. Spadaro, F. Frusteri, F. Arena, *J. Phys. Chem. B* 107 (2003) 6122–6130.
- [9] P. Bera, K.C. Ratil, V. Jayaram, G.N. Sublanna, M.S. Hegde, *J. Catal.* 196 (2000) 293–301.
- [10] D. Basu, S. Basu, *Int. J. Hydrogen Energy* 36 (2011) 14923–14929.
- [11] D. Basu, S. Basu, *Electrochim. Acta* 55 (2010) 5775–5779.
- [12] D. Basu, S. Sood, S. Basu, *Chem. Eng. J.* 228 (2013) 867–870.
- [13] N. Mano, F. Mao, A. Heller, *J. Am. Chem. Soc.* 124 (2002) 12962–12963.
- [14] Q. Wang, X. Cui, J. Chen, X. Zheng, C. Liu, T. Xue, H. Wang, Z. Jin, L. Qiao, W. Zheng, *RSC Adv.* 2 (2012) 6245–6249.
- [15] L.M. Lu, H.B. Li, F. Qu, X.B. Zhang, G.L. Shen, R.Q. Yu, *Biosens. Bioelectron.* 26 (2011) 3500–3504.
- [16] Y. Kuang, B.H. Wu, D. Hu, X. Zhang, J. chen, *J. Solid State Electrochem.* 16 (2012) 759–766.
- [17] T.T. Jiang, L.L. Yan, Y.Z. Meng, M. Xiao, Z.R. Wu, P. Tsiakaras, S.Q. Song, *Appl. Catal. B: Environ.* 162 (2015) 275–281.
- [18] A. Brouzgou, S.Q. Song, P. Tsiakaras, *Appl. Catal. B: Environ.* 158–159 (2014) 209–216.
- [19] L.L. Yan, A. Brouzgou, Y.Z. Meng, M. Xiao, P. Tsiakaras, S.Q. Song, *Appl. Catal. B: Environ.* 150–151 (2014) 268–274.
- [20] S.Q. Song, Y. Wang, P.K. Shen, *J. Power Sources* 170 (2007) 46–49.
- [21] H.Q. Li, G.Q. Sun, Q. Jiang, M.Y. Zhu, S.G. Sun, Q. Xin, *J. Power Source* 172 (2007) 641–649.
- [22] D.M. Gu, Y.Y. Chu, Z.B. Wang, Z.Z. Jiang, G.P. Yin, Y. Liu, *Appl. Catal. B: Environ.* 102 (2011) 9–18.
- [23] Y. Zhao, F. Wang, J. Tian, X. Yang, L. Zhan, *Electrochim. Acta* 55 (2010) 8998–9003.
- [24] V. Radmilovic, H.A. Gasteiger, P.N. Ross, *J. Catal.* 154 (1995) 98–106.
- [25] A. Bumajdad, M.I. Zaki, J. Eastoe, L. Pasupulety, *Langmuir* 10 (2004) 11223–11233.
- [26] C.S. Pan, D.S. Zhang, L.Y. Shi, *J. Solid State Chem.* 181 (2008) 1298–1306.
- [27] M. Holzinger, O. Vostrovsky, A. Hirsch, F. Hennrich, M. Kappes, R. Weiss, F. Jellen, *Angew. Chem. Int. Ed.* 40 (2001) 4002–4005.
- [28] F. Larachi, J. Pierre, A. Adnot, A. Bernis, *Appl. Surf. Sci.* 195 (2002) 236–250.
- [29] J. Zhao, W.X. Chen, Y.F. Zheng, *Mater. Chem. Phys.* 113 (2009) 591–595.
- [30] A. Brouzgou, L.L. Yan, S.Q. Song, P. Tsiakaras, *Appl. Catal. B: Environ.* 147 (2014) 481–489.
- [31] L. Feng, J. Yang, Y. Hu, J. Zhu, C. Liu, W. Xing, *Int. J. Hydrogen Energy* 37 (2012) 4812–4818.
- [32] T. Mori, D.R. Ou, J. Zou, J. Drennan, *Chin. Mater. Res. Soc.* 22 (2012) 561–571.
- [33] J. Wang, G. Rivas, M. Chicharro, *J. Electroanal. Chem.* 439 (1997) 55–61.
- [34] M.S. Gelej, G. Rivas, *Electroanalytical* 10 (1998) 771–775.